Influence of Yttria-Stabilized Zirconia on Microstructure and Electrical Properties of Doped Lanthanum Gallate

Talita Gishitomi Fujimoto[a]* [ID], Shirley Leite Reis[a], Eliana Navarro dos Santos Muccillo[a]

[a]Instituto de Pesquisas Energéticas e Nucleares, São Paulo, SP, Brasil

Lanthanum gallate with partial substitutions for strontium and magnesium shows higher ionic conductivity than traditional ionic conductors such as yttria-stabilized zirconia (8YSZ), and has been considered for application as solid electrolyte and electrode in Solid Oxide Fuel Cells operating at intermediate temperatures (500-700ºC). Parallel to the development of new solid electrolytes, improvement of the already known electrolytes has been one goal. In this work, the effects of adding 8YSZ to $La_{0.9}Sr_{0.1}Ga_{0.8}Mg_{0.2}O_{3-\delta}$ (LSGM), on the microstructure and electrical performance were investigated. Compound electrolytes consisting of up to 20 wt.% 8YSZ were prepared by solid state reactions. Sintered pellets with up to 10 wt.% 8YSZ achieved near full density after sintering at 1450ºC and reduction in the fraction of impurity phases. Addition of 8YSZ promoted grain growth to LSGM. The higher ionic conductivity was obtained for 1 wt.% 8YSZ addition with slight decrease of the apparent activation energy.

Keywords: *Lanthanum gallate, yttria-stabilized zircônia, microstructure, ionic conductivity.*

1. Introduction

Oxide-ion conductors with perovskite structure based on doped lanthanum gallate find application as solid electrolyte and electrodes in Solid Oxide Fuel Cells (SOFCs). These electrochemical devices have received considerable attention as clean-energy production systems, with several advantages, such as low noise, fuel flexibility, low emissions, high efficiency and cell scalability, compared to conventional energy conversion engines[1,2].

Since the pioneering works of Ishihara[3] and Feng[4], ceramic conductors consisting of lanthanum gallate with partial substitutions for strontium and magnesium in the A- and B-sites, respectively, of the perovskite structure ($La_{1-x}Sr_xGa_{1-y}Mg_yO_{3-\delta}$, with $0.1 \leq x,y \leq 0.2$) have been thoroughly investigated, due to their high ionic conductivity along with wide electrolytic domain, as described in recent reviews[5,6].

Among the studied compositions, the $La_{0.9}Sr_{0.1}Ga_{0.8}Mg_{0.2}O_{3-\delta}$ exhibits distorted perovskite structure with orthorhombic symmetry, high ionic conductivity and relatively low fraction of impurity phases[1,2,7,8].

Recently, the need to improve the physical properties of these ceramic solid electrolytes has led to the investigation of more complex systems constituted by two solid electrolytes (compound or composite electrolytes). In this context, few studies may be found related to doped lanthanum gallates. Addition of small amounts of $La_{0.8}Sr_{0.2}Ga_{0.8}Mg_{0.2}O_{3-\delta}$ to $Ce_{0.9}Gd_{0.1}O_{1.95}$ resulted in an expanded electrolytic domain towards low oxygen partial pressures[9]. Improvement on the ionic conductivity was observed by addition of 9 mol% yttria-stabilized zirconia to $La_{0.9}Sr_{0.1}Ga_{0.8}Mg_{0.2}O_{2.85}$[10]. Unit SOFCs with composite electrolytes of $La_{0.85}Sr_{0.15}Ga_{0.8}Mg_{0.2}O_{2.825}$ and $Ce_{0.85}Sm_{0.15}O_{1.925}$ did not show significant enhancement compared to the single electrolyte component cell[11].

In this work a systematic study of LSGM - 8YSZ compound electrolytes was carried out, aiming to correlate the microstructure and the ionic conductivity.

2. Experimental

2.1 Materials

Lanthanum oxide, La_2O_3 (99.9%, **Alfa Aesar, USA**), gallium oxide, Ga_2O_3 (99.99%, **Alfa Aesar, USA**), strontium carbonate, $SrCO_3$ (99.99%, **Alfa Aesar, USA**) and MgO (P.A., **Merck, German**) were used as starting materials to synthesize the composition $La_{0.9}Sr_{0.1}Ga_{0.8}Mg_{0.2}O_{3-\delta}$. Commercial 8YSZ (99.6%, **Tosoh, Japan**) was used to prepare compound electrolytes of (100-x)LSGM + x8YSZ with x=0, 1, 10 and 20 wt.%.

2.2 Preparation methods

LSGM was synthesized by the solid state reaction method. At first, lanthanum oxide precursor was heat treated at 1000ºC for 3 h. Stoichiometric amounts of the starting materials were mixed together, calcined at 1250ºC for 4 h and desagglomerated in an agate mortar with pestle. This procedure was repeated twice amounting 12 h of calcination. Afterwards, the powder mixture was attrition milled with zirconia media and isopropyl alcohol for 1 h, followed by drying at 40ºC. This procedure was found to produce dense specimens after sintering at 1450ºC[12].

*e-mail: talita.fujimoto@usp.br

Compound solid electrolytes were prepared by mixing together desired amounts of the synthesized LSGM and commercial 8YSZ in agate mortar with isopropyl alcohol until drying. The mixtures were pressed (50 MPa) into pellets in a stainless steel dye. Sintering of green compacts was carried out in a resistive furnace (Lindberg BlueM) in air at temperatures ranging from 1350 to 1450ºC for 4 h.

2.3 Characterization methods

The crystalline structure of powder mixtures and sintered pellets was evaluated by X-ray diffraction, XRD (Bruker-AXS, D8 Advance) in the $20º \leq 2\theta \leq 80º$ angular range with 0.05º step size and 2 s counting time, using Ni-filtered Cu K_α radiation ($\lambda=1.5405$ Å). Identification of crystalline phases was accomplished by comparing the experimental diffraction patterns with those of powder diffraction files (ICSD). The apparent density (ρ) of sintered specimens was determined by the water immersion method. The relative density (ρ_r) was calculated from:

$$\rho_r = \left(\frac{\rho}{\rho_c}\right).100 \tag{1}$$

where ρ_c is the density of the compound electrolyte given by:

$$\rho_c = \rho_1 V_1 + \rho_2 V_2 \tag{2}$$

and ρ_i and V_i (i=1, 2) are the crystallographic densities and volume fractions of phases 1 (LSGM) and 2 (8YSZ), respectively, in weight percent.

Microstructure features were observed by field emission gun scanning electron microscopy, FEG-SEM (Inspect F50, FEI). In this case, the powders were spread out onto carbon tape and sintered pellets were polished with diamond pastes (15, 6 and 1 μm) and thermally etched at 100ºC below the sintering temperature. The average grain size was estimated by the intercept method[13].

Ionic conductivity measurements were carried out in an impedance analyzer (4192A, Hewlett Packard) in the 5 Hz to 13 MHz frequency range with 200 mV of applied voltage. Silver paste was applied onto parallel surfaces of sintered pellets and fired at 400ºC to remove the organic binder.

3. Results and Discussion

Figure 1 shows powder XRD patterns collected during preparation of LSGM. The diffraction pattern of the starting mixture shows, as expected, the main peaks of lanthanum (1) and gallium (2) oxides. After the first calcination step at 1250ºC for 4 h, the LSGM phase (indicated by *) has already been formed. Nevertheless, as the reaction among the several starting materials is incomplete, some diffraction peaks of impurity phases are detected, especially $La_4Ga_2O_9$ (3), $LaSrGa_3O_7$ (4) and $LaSrGaO_4$ (5). The subsequent steps of calcination and attrition milling promoted a decrease in the relative fraction of undesired phases, such that the final

powder mixture consists primarily of the LSGM phase and minor amounts (less than 5%, estimated by intensity ratios) of the usually observed impurity phases.
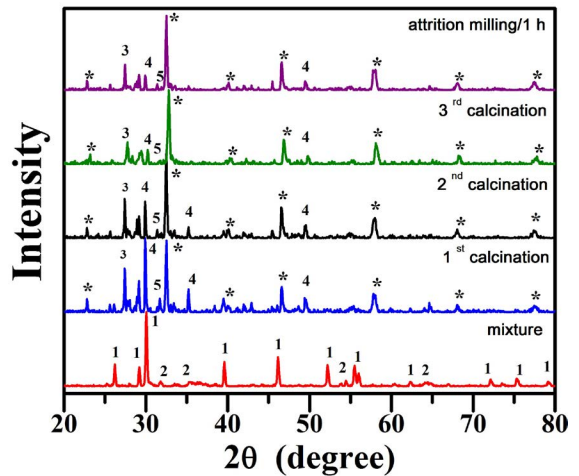

Figure 1. XRD patterns of the starting powder mixture and after calcination (1250 ºC for 4 h) and attrition milling. 1 - La_2O_3, 2 - Ga_2O_3, 3 - $La_4Ga_2O_9$, 4 - $LaSrGa_3O_7$ and 5 - $LaSrGaO_4$. The orthorhombic phase of LSGM is indicated by *.

FEG-SEM micrographs of (a) as-prepared LSGM, (b) 8YSZ commercial powder and (c) 8YSZ with 20 wt.% LSGM are depicted in Figure 2. The LSGM powder (Figure 2a) prepared by solid state reaction is characterized by agglomerated particles of irregular shape. Commercial 8YSZ (Figure 2b) are spherical granules resulting from the spray drying process in the production route. The mixture of 8YSZ and LSGM (Figure 2c) consists of porous agglomerates, their size increasing with increasing 8YSZ content. These agglomerates seems to be soft, they break during the conformation step, leading to high density pellets after sintering at 1450ºC, as summarized in Table 1.

The relative density of pure LSGM sintered at 1350ºC is 93.5%. In contrast, for higher sintering temperatures the density is 99%. The relative density of compound electrolytes decreases for increasing 8YSZ addition. At 1450ºC, the density is near full for all pellets except for those with 20 wt.% 8YSZ. The density of common impurity phases was not taken into account in these calculations, because their total amount is relatively low. Hereafter only results on pellets sintered at 1450ºC will be shown.

XRD patterns of as-sintered pellets are shown in Figure 3. The plots on the left exhibit the entire angular range of XRD measurements, whereas those on the right are enlarged views of the 24-32º range, where the main diffraction peaks of impurity phases are detected. 8YSZ and LSGM display the characteristic cubic fluorite-type and orthorhombic perovskite-type crystalline structures, respectively. Surprisingly, addition of 8YSZ to LSGM promotes phase stabilization, and for 10 wt.% addition, the XRD pattern resembles that of a single phase material. Increasing the fraction of 8YSZ to 20 wt.% a new phase attributed to lanthanum zirconate, $La_2Zr_2O_7$ with pyrochlore structure was detected revealing a strong interaction among the individual elements of the compound electrolyte.
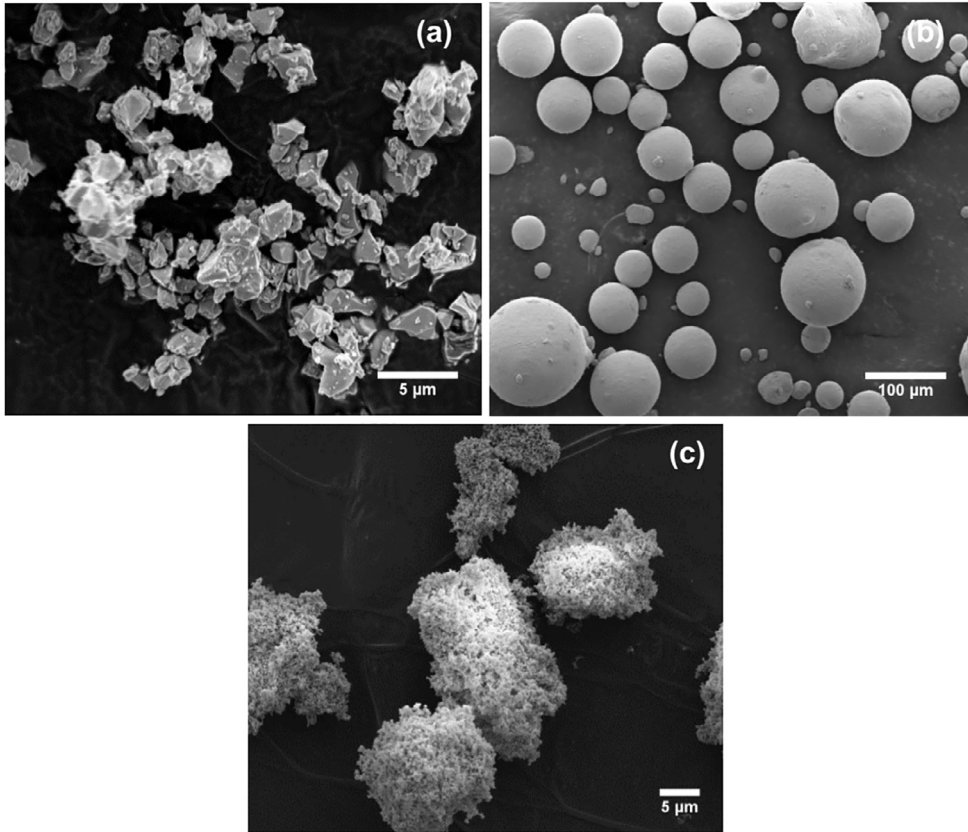
Figure 2. FEG-SEM micrographs of (a) LSGM, (b) 8YSZ and (c) 20 wt.% 8YSZ added to LSGM.
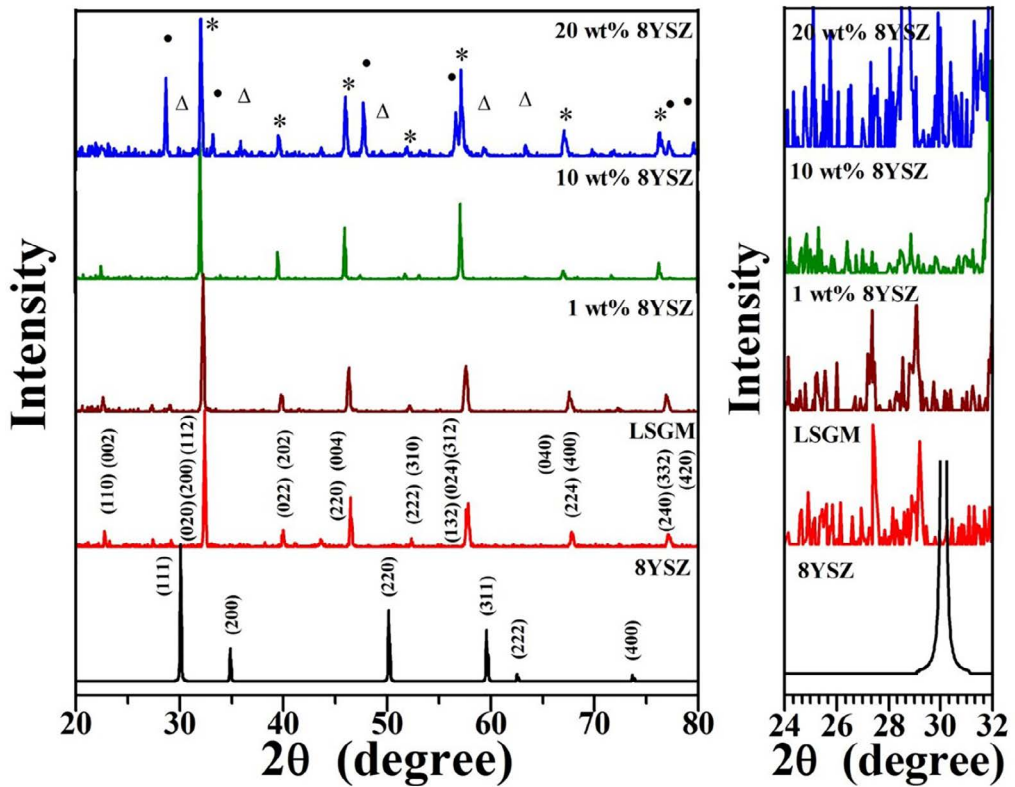

Figure 3. XRD patterns of LSGM, 8YSZ and compound electrolytes after sintering at 1450 °C for 4 h. * - LSGM, Δ - 8YSZ and • - La$_2$Zr$_2$O$_7$.

Table 1. Values of relative density (ρ_r) for LSGM pellets containing different amounts of 8YSZ and sintered at several temperatures for 4 h.

Sintering Temperature(ºC)	8YSZ(wt.%)	ρ_r(%)
1350	0	93.5
1350	1	96.0
1350	10	71.0
1350	20	74.6
1400	0	≈99
1400	1	≈99
1400	10	85.5
1400	20	85.0
1450	0	≈99
1450	1	≈99
1450	10	≈99
1450	20	92.3

Figure 4 shows FEG-SEM micrographs of polished and thermally etched sintered pellets of (a) LSGM, (b) 8YSZ, (c) LSGM+10 wt.% 8YSZ, and (d) LSGM+20 wt.% 8YSZ. The main microstructure features of LSGM (Figure 4a) are polygonal grains with negligible porosity. Grains with smooth and rough surfaces are observed. Similar features are found for 8YSZ (Figure 4b) pellets with grains with smooth surfaces. This difference in the texture of LSGM grains has already been reported and attributed to different factors, such as the presence of stacking faults, or to changes in the microstructure occurring during thermal etching or during cooling down from the sintering temperature[14-17]. The compound electrolytes exhibit similar features as those of base ceramic materials, except by microregions with a different (dark) contrast suggesting the emerging of a new phase. These findings are in general agreement with XRD results, which revealed the lanthanum zirconate as a second phase in these ceramics. The FEG-SEM results shows inequivocally that this secondary phase had already been formed with 10 wt.% 8YSZ addition to LSGM. Values of the average grain size of sintered pellets are summarized in Table 2.
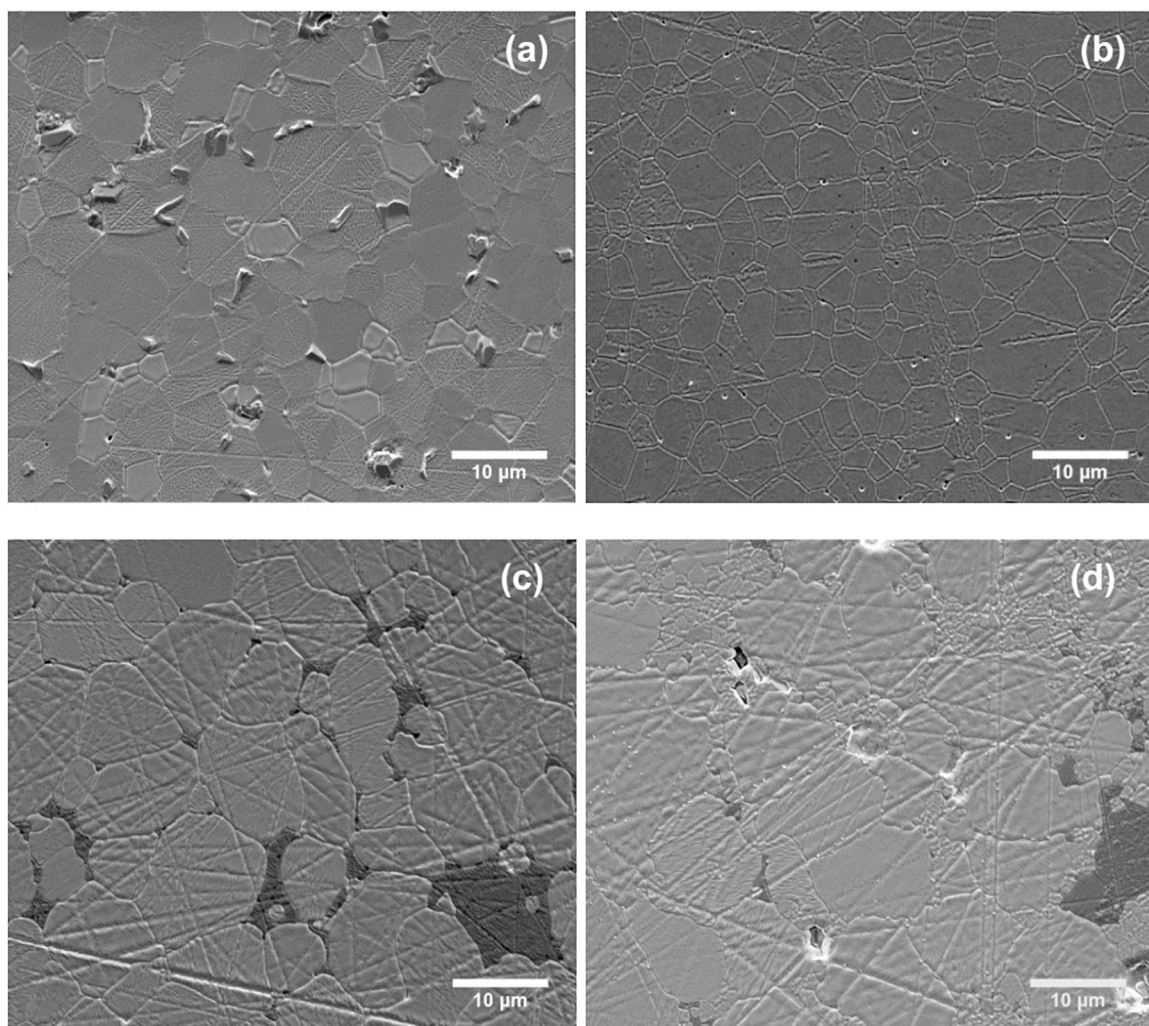

Figure 4. FEG-SEM micrographs of (a) LSGM, (b) 8YSZ, (c) 10 wt.% and (d) 20 wt.% 8YSZ added to LSGM.

Table 2. Values of average grain size and apparent activation energy (E_a) for conduction of solid electrolytes sintered at 1450 ºC for 4 h.

8YSZ(wt.%)	Average grain size (μm)	E_a(eV)
0	6.35	0.99
1	7.15	0.98
10	11.48	0.93
20	13.30	1.02

The average grain size of LSGM is 6.35 μm, which is close to that of pure 8YSZ (5.55 μm) sintered under the same experimental conditions. Addition of 8YSZ to LSGM produced substantial grain growth, suggesting a strong interaction between these two solid electrolytes during sintering. The grain growth process is fast up to 10 wt.% 8YSZ and slows down for higher additive contents.

Impedance spectroscopy diagrams recorded at 268ºC are shown in Figure 5. The real (Z') and the imaginary (Z'') components of the total impedance were normalized for pellet dimensions for comparison purpose. Numbers in these plots are the relaxation frequencies. As usual for oxide-ion conductors, the whole diagram consists of decentralized arcs, ascribed to the resistive and capacitive effects of grains, grain boundaries and the electrolyte/electrode interface[18]. The impedance diagrams of pure LSGM and LSGM with 1 wt.% 8YSZ show two arcs at high and low frequencies. The arc attributed to the grain boundaries, which is usually detected at intermediate frequencies (~ 1 kHz), becomes significant in polycrystalline ceramics only for grain sizes lower than 5 μm[19]. Then, only the grain or bulk component of the total conductivity was analyzed. The bulk resistivity of LSGM with 1 wt.% 8YSZ is slightly lower than that of pure LSGM. In contrast, addition of 10 wt.% 8YSZ resulted in a huge increase of the bulk resistivity.
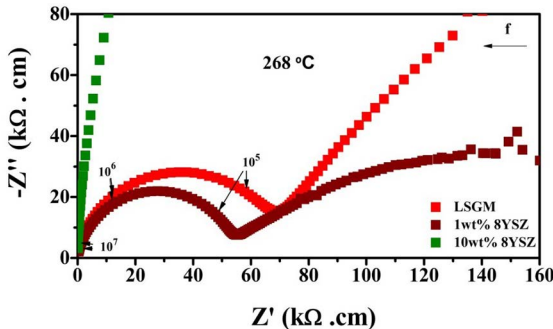
Figure 5. Impedance spectroscopy diagrams of pure LSGM and with 1 and 10 wt.% addition of 8YSZ. Temperature of measurement = 268ºC.

Arrhenius plots of the bulk conductivity of sintered pellets are depicted in Figure 6. The straight lines are the fitting of experimental points. Indeed, the addition of 1 wt.% 8YSZ to LSGM resulted in a small increase of the bulk conductivity of LSGM. The apparent activation energy values determined by curve fitting are summarized in Table 2.
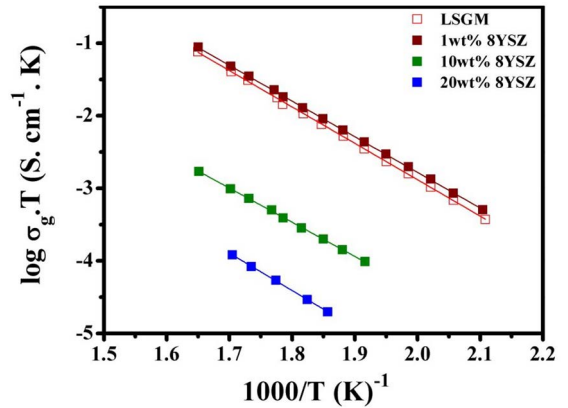
Figure 6. Arrhenius plots of the bulk conductivity of solid electrolytes sintered at 1450 ºC for 4 h.

Addition of up to 10 wt.% 8YSZ to LSGM promoted decrease of the apparent activation energy for the bulk conductivity.

The grain size (Table 2) does not influence the bulk conductivity of polycrystalline solid electrolytes. In contrast, the density or porosity (Table 1) may reduce drastically the ionic conductivity. The specimen with 20 wt.% 8YSZ, for example, exhibits the lowest bulk conductivity (Fig. 6), which is a consequence of the difference in the conductivity of both electrolytes, and the presence of the insulating phase ($La_2Zr_2O_7$), and because of its lower density compared to other specimens.

The overall results suggest that adding 8YSZ to LSGM may improve some properties. From a microstructural point of view, additions up to 10 wt.% 8YSZ promotes better phase stability, by decreasing the impurity phases contents. Moreover, 1 wt.% 8YSZ added to LSGM results in a small and unexpected (the ionic conductivity of 8YSZ is known to be much smaller than that of LSGM) increase of the bulk conductivity of LSGM. The reason as to why this occurs is unclear, but it seems to be related to a decrease in the apparent activation energy for conduction, related to improved stoichiometry of LSGM as a consequence of reduction of impurity phase contents. Interaction between the two solid electrolytes takes place during sintering, giving rise to lanthanum zirconate as secondary phase. That phase with pyrochlore structure has lower ionic conductivity than both LSGM and 8YSZ[20].

4. Conclusions

Compound electrolytes constituted by mixtures of doped lanthanum gallate and yttria-stabilized zirconia were successfully prepared by solid state reaction. Additions of up to 10 wt.% 8YSZ reduce the fraction of impurity phases in the LSGM. Interaction of the two electrolytes gives rise to lanthanum zirconate as secondary phase for additions of at least 10 wt.% 8YSZ. A small increase of the bulk conductivity of LSGM was observed for 1 wt.% 8YSZ addition, with a decrease of the apparent activation energy for conduction.

5. Acknowledgements

6. References

1. Minh NQ. Ceramic Fuel Cells. *Journal of the American Ceramic Society*. 1993;76(3):563-588.

2. Gao Z, Mogni LV, Miller EC, Railsback JG, Barnett SA. A perspective on low-temperature solid oxide fuel cells. *Energy & Environmental Science*. 2016;9(5):1602-1644.

3. Ishihara T, Matsuda H, Takita Y. Doped LaGaO$_3$ Perovskite Type Oxide as a New Oxide Ionic Conductor. *Journal of the American Chemical Society*. 1994;116(9):3801-3803.

4. Feng M, Goodenough JB. A superior oxide-ion electrolyte. *European Journal of Solid State and Inorganic Chemistry*. 1994;31:663-672.

5. Yokokawa H, Sakai N, Horita T, Yamaji K, Brito ME. Solid Oxide Electrolytes for High Temperature Fuel Cells. *Electrochemistry*. 2005;73(1):20-30.

6. Morales M, Roa JJ, Tartaj J, Segarra M. A review of doped lanthanum gallates as electrolytes for intermediate temperature solid oxides fuel cells: From materials processing to electrical and thermo-mechanical properties. *Journal of the European Ceramic Society*. 2016;36(1):1-16.

7. Huang PN, Petric A. Superior Oxygen Ion Conductivity of Lanthanum Gallate Doped with Strontium and Magnesium. *Journal of the Electrochemical Society*. 1996;143(5):1644-1648.

8. Liu N, Shi M, Wang C, Yuan YP, Majewski P, Aldinger F. Microstructure and ionic conductivity of Sr- and Mg-doped LaGaO$_3$. *Journal of Materials Science*. 2006;41(13):4205-4213.

9. Jo SH, Muralidharan P, Kim DK. Electrical conductivity studies on the LSGM-CGO composite electrolytes. *Journal of Alloys and Compounds*. 2010;491(1-2):416-419.

10. Raghvendra, Singh RK, Singh P. Electrical conductivity of LSGM-YSZ composite materials synthesized via coprecipitation route. *Journal of Materials Science*. 2014;49(16):5571-5578.

11. Wu YC, Lee MJ, Li X. Analysis of the microstructure and physical properties of La$_{0.85}$Sr$_{0.15}$Ga$_{0.8}$Mg$_{0.2}$O$_{2.825}$ and Ce$_{0.85}$Sm$_{0.15}$O$_{1.925}$ composite electrolytes used in solid oxide fuel cells. *Journal of the European Ceramic Society*. 2015;35(16):4485-4495.

12. Reis SL, Muccillo ENS. Preparation of dense La$_{0.9}$Sr$_{0.1}$Ga$_{0.8}$Mg$_{0.2}$O$_{3-\delta}$ with high ionic conductivity by solid-state synthesis. *Ionics*. 2018;24(6):1693-1700.

13. Mendelson MI. Average Grain Size in Polycrystalline Ceramics. *Journal of the American Ceramic Society*. 1969;52(8):443-446.

14. Zhao X, Li X, Xu N, Huang K. Beneficial effects of Mg-excess in La$_{1-x}$Sr$_x$Ga$_{1-y}$Mg$_{y+z}$O$_{3-\delta}$ as solid electrolyte. *Solid State Ionics*. 2012;214:56-61.

15. Wu YC, Lee MZ. Properties and microstructural analysis of La$_{1-x}$Sr$_x$Ga$_{1-y}$Mg$_y$O$_{3-\delta}$ solid electrolyte. *Ceramics International*. 2013;39(8):9331-9341.

16. Stevenson JW, Armstrong TR, Pederson LR, Li J, Lewinsohn CA, Baskaran S. Effect of A-site cation nonstoichiometry on the properties of doped lanthanum gallate. *Solid State Ionics*. 1998;113-115:571-583.

17. Oncel C, Ozkaya B, Gulgun MA. X-ray single phase LSGM at 1350 ºC. *Journal of the European Ceramic Society*. 2007;27(2-3):599-604.

18. Bauerle JE. Study of solid electrolyte polarization by a complex admittance method. *Journal of Physics and Chemistry of Solids*. 1969;30(12):2657-2670.

19. Kleitz M, Bernard H, Fernandez E, Schouler E. Impedance spectroscopy and electrical resistance measurements on stabilized zirconia. In: Heuer AH, Hobbs LW, eds. *Science and Technology of Zirconia*. Westerville: The American Ceramic Society; 1981. p. 310-336.

20. Mahato N, Banerjee A, Gupta A, Omar S, Balani K. Progress in material selection for solid oxide fuel cell technology: A review. *Progress in Materials Science*. 2015;72:141-337.